JOURNAL OF MAGNETIC RESONANCE **127,** 184–191 (1997)
ARTICLE NO. MN971190

Model-Free Approach beyond the Borders of Its Applicability

Dmitry M. Korzhnev, Vladislav Yu. Orekhov, and Alexander S. Arseniev

Shemyakin and Ovchinnikov Institute of Bioorganic Chemistry, Russian Academy of Sciences, Ul. Miklukho-Maklaya 16/10, Moscow 117871, Russia

Received December 23, 1996; revised May 15, 1997

Model calculations presented in this article show that commonly used methodology of ^{15}N relaxation data analysis completely fails in detecting nanosecond time scale motions if the major part of the molecule is involved in these motions. New criteria are introduced for the detection of such cases, based on the dependence of the apparent overall correlation time, derived from the T_1/T_2 ratio, on the spectrometer frequency. Correctly estimating the overall rotation correlation time τ_R was shown to play the key role in model-free data analysis. It is found, however, that in cases of slow internal motions with characteristic times of more than 3–4 ns, the effective τ_R provided by the T_1/T_2 ratio for individual amide nitrogens can be used for the characterization of the fast picosecond internal dynamics. © 1997 Academic Press

INTRODUCTION

Internal motions of macromolecules are of fundamental importance for their biological functions, stability and folding. ^{15}N and ^{13}C NMR relaxation measurements provide unique experimental data for the characterization of intramolecular motions in a wide range of time scales from pico- to milliseconds. The experimental transverse and longitudinal relaxation rates and NOEs can be expressed in terms of the spectral density function $J(\omega)$, which is the Fourier transform of the reorientation correlation function $C(t)$. Commonly, the experimental data are interpreted using the original (*1, 2*) or the extended (*3*) ''model-free'' approach, which provides order parameters and correlation times as the spatial and temporal measures of the internal motions. Although many modifications were proposed (*4, 5*) for heteronuclear ^{15}N and ^{13}C relaxation data analysis described by Kay *et al.* (*6*), the main line remains the same. The simplest form of the model-free spectral density function is applied first. Only for those particular nuclei for which experimental data could not be satisfactorily fitted by the simple form of $J(\omega)$ is the more general expression with a greater number of parameters applied.

However, one should always keep in mind that the good fit between experiment and model only means that this particular model could not be rejected, and can in no sense exclude other reasonable models. This is of particular importance if the alternative model assumes qualitatively different behavior of the system under consideration. The simplest form of the spectral density function (*1*) assumes isotropic molecular rotational tumbling and fast internal motions with characteristic times shorter than 100 ps. The alternative and more complicated models account also for the possible anisotropy of the overall molecular rotational diffusion (*7*) or for slow internal motions (*3*). As was shown in our previous work (*8*), the same relaxation data can satisfactorily fit the simple (*1, 2*) and extended (*3*) forms of the spectral density function, leading to qualitatively different pictures of the protein internal dynamics. In the latter case, the lower order parameters and longer overall rotational correlation times are observed.

Model calculations presented in this article address the following question. What misinterpretations of internal motions could be introduced by the commonly used formal statistical approach if one of the assumptions of the simplest form of the model-free spectral density function is not valid? In particular we unambiguously show that the commonly used methodology of relaxation data analysis leads to erroneous conclusions about the characteristics of internal motions if the major part of the molecule is involved in the nanosecond time scale motions. New criteria based on relaxation data at different spectrometer fields are proposed for the detection of such cases.

THEORY AND METHODS

To extract the parameters of internal motions from the experimental NMR data one needs models both for the overall rotation and for the internal motions of the molecule. Current NMR techniques provide 1–5% uncertainty in the determination of the order parameters within the frame of the particular models of the overall and internal motions (*4, 9*). However, the real accuracy of the extracted characteristics of internal motion depends both on the uncertainties of the experimental relaxation data and on the model chosen for their interpretation. Thus, calculations of Schurr *et al.* (*10*) show that using the extended model-free (*3*) form of the spectral density function can result in substantial amplitudes of nonexistent internal motions on the nanosecond time scale due to erroneous neglect of the anisotropy of molecular

1090-7807/97 $25.00

tumbling. Orekhov *et al.* (*8*) showed that in some cases the same experimental relaxation data can be well fitted by both simple (*1*) and extended (*3*) model-free formulas, leading to substantially different parameters of internal motions. Therefore, clear criteria of the selection between the different models of overall and internal molecular motions are required.

Relaxation Data and ''Model-Free'' Formalism

A typical set of heteronuclear NMR relaxation data consists of longitudinal [$R(S_z)$] and transverse [$R(S_x)$] relaxation rates and heteronuclear NOEs measured at one or several spectrometer frequencies. Basic NMR techniques for measuring these quantities are described by Kay *et al.* (*6*).

The relaxation of a spin-$\frac{1}{2}$ X nucleus in the two-spin X–^{1}H system (e.g., amide ^{15}N–^{1}H or ^{13}C–^{1}H in proteins) is governed by two dominant mechanisms. The first is the relaxation due to the dipole–dipole interaction between the X nucleus and the directly attached proton. The second is due to the chemical-shift anisotropy (CSA). It is necessary also to account for the contribution of other pseudo-first-order processes, such as conformational exchange (*11*) to the transverse relaxation rate $R(S_x)$. The experimental transverse and longitudinal relaxation rates and NOEs can be expressed in terms of the spectral density function $J(\omega)$, which is the Fourier transform of the reorientation correlation function $C(t)$ (*12*). In general one should distinguish the correlation functions for the heteronuclear dipole–dipole interaction associated with the reorientation of the X–^{1}H vector and the correlation function of the axis of the auxiliary symmetric CSA tensor. Fortunately, however, the CSA axis and the ^{15}N–^{1}H vector are almost parallel, which allows interpretation of the relaxation data assuming the same correlation function for both interactions.

If the particular form of the correlation function is chosen, spatial and temporal characteristics of internal and overall motions are obtained as adjustable parameters by minimizing the target function

$$\chi^2(\zeta) = \sum_{i=1}^{N} \frac{(V_i^{\text{th}}(\zeta) - V_i^{\text{exp}})^2}{(\Delta V_i^{\text{exp}})^2}, \qquad [1]$$

where $V^{\text{th}}(\zeta)$ and V^{exp} are the theoretical and experimental values, respectively, ΔV^{exp} is the uncertainty of the experimental value, index i runs over the set of relaxation rates and NOEs, N is the number of experimental values, and ζ denotes the set of extracted motional parameters (which can include the conformational exchange term Δ_{ex}).

If internal motions are not correlated with the overall rotation of the molecule and the overall molecular rotation is isotropic, the total correlation function $C(t)$ can be rigorously factored into a product of internal $C_{\text{I}}(t)$ and overall $C_{\text{O}}(t)$ parts (*1*):

$$C(t) = C_{\text{I}}(t)C_{\text{O}}(t). \qquad [2]$$

Although the above factorization is not always valid for the case of anisotropic overall rotation it is shown to be a good approximation (*2, 10, 13*) and is implied in the subsequent consideration.

A relatively wide set of physical processes connected with the internal molecular motions on the picosecond and nanosecond time scales can be described by the purely diffusive, multiexponential form of the autocorrelation function (*14*). In the original model-free formalism (*1, 2*), the internal motions are characterized by the time constant τ_{e} and generalized order parameter S^2 without any assumptions about the nature of the motions. The main assumption of this model is that all internal motions are in the extreme narrowing limit; i.e., their characteristic correlation times are much shorter than the overall rotation correlation time. The corresponding autocorrelation function is given by

$$C_{\text{I}}(t) = S^2 + (1 - S^2)\exp(-t/\tau_{\text{e}}). \qquad [3a]$$

In the subsequent analysis, this model will be referred to as the ''fast I'' (S^2, τ_{e}) model. An even simpler form of the autocorrelation function corresponding to a very small value of τ_{e} is often used:

$$C_{\text{I}}(t) = S^2. \qquad [3b]$$

In the subsequent analysis this model will be referred to as the ''fast II'' (S^2) model.

One of the simplest forms of the autocorrelation function accounting for the motions on the time scale close to the correlation time of molecular Brownian rotation was introduced by Clore *et al.* (*3*). Usage of this correlation function is usually referred to as the extended model-free approach. It assumes the presence of two uncorrelated sets of internal motions—fast, described by the correlation time τ_{f} and order parameter S_{f}^2, and intermediate, with correlation time τ_{s} and order parameter S_{s}^2. The corresponding expression for the autocorrelation function is given by

$$C_{\text{I}}(t) = S_{\text{f}}^2 S_{\text{s}}^2 + (1 - S_{\text{f}}^2)\exp(-t/\tau_{\text{f}}) + (S_{\text{f}}^2 - S_{\text{f}}^2 S_{\text{s}}^2)\exp(-t/\tau_{\text{s}}). \qquad [4a]$$

Here the order parameter S^2 of Eqs. [3] is a multiple of S_{f}^2 and S_{s}^2. If $S_{\text{s}}^2 = 1$, Eq. [4] reduces to Eqs. [3]. To minimize the number of adjustable model parameters, in most cases the second term in Eq. [4a] including τ_{f} is omitted, assuming a very small value of τ_{f}:

$$C_{\text{I}}(t) = S_{\text{f}}^2 S_{\text{s}}^2 + (S_{\text{f}}^2 - S_{\text{f}}^2 S_{\text{s}}^2)\exp(-t/\tau_{\text{s}}). \qquad [4b]$$

In the subsequent analysis this model will be referred to as the ''intermediate'' or ''nanosecond'' (S_f^2, S_s^2, τ_s) model.

Models of the Overall Rotation

The simplest, isotropic, model of overall rotation implies that the molecule undergoing rotational Brownian diffusion has an almost spherical shape. In this case the overall correlation function can be represented in the single-exponential form

$$C_O(t) = \exp(-t/\tau_R), \qquad [5]$$

where τ_R is the overall-rotation correlation time.

The correlation function of the overall rotation of anisotropic molecules is described by a more complex expression. According to Woessner's model (*7*), the relaxation in rigid [$C_I(t) = 1, C(t) = C_O(t)$] anisotropic molecules undergoing rotational Brownian diffusion is governed by the five-exponential correlation function which reduces to a three-exponential form in the case of axially symmetric top molecules:

$$\begin{aligned} C(t) &= A\exp(-t/\tau_a) + B\exp(-t/\tau_b) + C\exp(-t/\tau_c) \\ \tau_a &= (4D_\parallel + 2D_\perp)^{-1}, \quad \tau_b = (D_\parallel + 5D_\perp)^{-1}, \\ \tau_c &= (6D_\perp)^{-1} \\ A &= (3/4)\sin^4\theta, \quad B = 3\sin^2\theta\cos^2\theta, \\ C &= (3\cos^2\theta - 1)/2. \end{aligned} \qquad [6]$$

Here $D_\perp$ and $D_\parallel$ are eigenvalues of the diffusion tensor for an axially symmetric body, and θ denotes the angle between the internuclear vector and the symmetry axis of the molecule.

For the sake of convenience in the following consideration, for the description of the overall rotation behavior of axially symmetric anisotropic molecules we use another set of parameters: angle θ, ratio of diffusion rates $D_\parallel/D_\perp$, and the effective rotation correlation time, τ_R, defined as

$$\tau_R = (4D_\perp + 2D_\parallel)^{-1}. \qquad [7]$$

For isotropic overall rotation, all three correlation times (Eq. [6]) become equal to the effective correlation time τ_R given by Eq. [7], and the correlation functions given by Eq. [6] are reduced to the single-exponential form (Eq. [5]).

Simulation of Relaxation Data

To sample the effects caused by the internal motions on the nanosecond time scale on the results of regular relaxation data analysis, we have simulated a set of relaxation data corresponding to isotropic overall molecular tumbling (Eq. [5]) and the nanosecond model of internal motions (Eq. [4b]). Although simulated relaxation data were used as they are without any noise, for the calculation of the loss function (Eq. [1]) the following uncertainties were ascribed: 2% for $R(S_x)$ and $R(S_z)$ values and 3% for NOE. This corresponds to the most precise experimental data published by now.

In the following, the exact model parameters are noted as in Eqs. [3]–[5], [6], and [7]. Apparent parameters of internal dynamics obtained by model fitting are designated by the subscript ''app,'' e.g., $(S^2)_{app}$. All calculations of relaxation data were performed using homebuilt software DASHA3.3 (*15*).

Overall-Rotation Correlation Times

As is shown below, τ_R is the key parameter for the proper interpretation of the relaxation data. Usually an initial guess of τ_R in the analysis of $^1H-^{15}N$ backbone dynamics is obtained from the $R(S_x)/R(S_z)$ ratio (*6*). Subsequently τ_R is refined by averaging on those residues, which exhibit high order parameter, small τ_e value and relatively high $^1H-^{15}N$ NOE. In all our computations we used apparent $(\tau_R)_{app}$ values obtained from the $R(S_x)/R(S_z)$ ratio except those specially noted cases where we utilize exact values. Since calculations were made for the single $^1H-^{15}N$ vector without averaging over different residues, the results obtained for the internal motions on the nanosecond time scale imply either that the analysis is performed for the individual $^1H-^{15}N$ pairs or that most of the residues in the molecule are involved in the same motions and consequently averaging of the $R(S_x)/R(S_z)$ ratio is appropriate.

Statistical Criterion of the Selection between the Models

In the model selection, we mostly followed the strategy described by Mandel *et al.* (*5*). Namely, extensive Monte Carlo numerical simulations were performed to estimate the probability distribution for statistics characterizing the goodness of the fit between the dynamic models and the simulated relaxation data. The model is assumed statistically approved if it provides a target function value that is less than the critical value. The critical value corresponds to a 0.05 probability of obtaining the target function greater than this value by chance. Choosing the 0.1 probability critical level or using the *F*-statistics criterion (*5*) leads to minor differences in the results of the calculations (data not shown) and consequently does not affect our conclusions. Since noise-free simulated data are used in model fitting, the values of the loss function obtained should be regarded as the possible contribution due to using the wrong spectral density function model into the loss function one can expect in practice. That is, the wrong model would be rejected only if this contribution is close to or higher than the critical value.

RESULTS AND DISCUSSION

Discrimination between ''Fast'' and ''Nanosecond'' Models

It is generally accepted that proteins exhibit motions on a wide range of time scales from femtoseconds to hours. If chemical exchange is neglected, NMR relaxation is sensitive to the motions in the picosecond–nanosecond time scale. The upper temporal cutoff for the motions, which affects the relaxation rates and NOEs, is provided by the correlation time of the overall molecular rotation. However, the methodology commonly used in the $^{15}N-^{1}H$ NMR dynamic relaxation studies from the very beginning implies the absence of nanosecond motions for most of the protein. This assumption is implicit if Eqs. [3] are utilized for the determination of the overall-rotation correlation time. Namely, the fast II (Eq. [3b]) model is implied if τ_R is calculated from the $R(S_x)/R(S_z)$ ratio (*6*). Alternatively fast I or fast II models are used if τ_R is obtained by the minimization of the total loss function which is the sum of loss functions (Eq. [1]) for individual $^{15}N-^{1}H$ vectors. However, if there are significant motions on the nanosecond time scale throughout the protein, τ_R provided by the $R(S_x)/R(S_z)$ ratio or as a result of total-loss-function minimization is underestimated. Orekhov *et al.* (*8*) note that in the subsequent model-free analysis, this underestimated τ_R provides a good fit of the experimental data to the fast I and fast II models of internal motions (Eqs. [3]) and leads to an erroneous conclusion about the nature of internal dynamics. Therefore, the problem of discrimination between fast and nanosecond models of protein internal dynamics is coupled with the determination of the τ_R value.

Indeed results of several recent publications point to possible τ_R underestimation in the regular model-free analysis. In particular contradictions were reported between ^{13}CO and ^{15}N relaxation data for cytochrome C2 (*16*) and T4 lysozyme (*17*). In both cases the overall correlation time obtained in the $^{1}H-^{15}N$ relaxation study lead to unphysically high order parameters for a number of $^{13}CO-^{13}C^{\alpha}$ vectors. Besides, results on $^{13}C-^{1}H$ methyl relaxation in human ubiquitin (*18*) correspond poorly to the rotation correlation time derived from the ^{15}N $R(S_x)/R(S_z)$ ratio; i.e., order parameters of several methyls were higher than the Woessner limit (0.111). Mismatch of NH order parameters obtained in the model-free analysis of experimental relaxation data and those obtained in long (1 ns) MD of solvated hen lysozyme was observed (*19*) with MD order parameters being smaller. Using a new modification of the spectral density mapping approach for ^{15}N relaxation data analysis, Lefevre *et al.* (*20*) found nanosecond motions for almost all residues in the dimerization domain of GAL4. All these results suggest that in the analysis of macromolecular relaxation data, one should pay much attention to the possible existence of nanosecond internal motions.

Besides NMR there are numerous methods which provide values of molecular overall-rotation correlation times. They are depolarized light scattering, time-resolved fluorescence depolarization, hydrodynamic calculations, etc. However, results presented in different publications can vary significantly. For example, for lysozyme, a correlation time of 8.3 $\pm$ 0.3 ns (adjusted to 20°C) was obtained in a ^{15}N relaxation study (*21*). Depolarized light scattering provides τ_R = 10.0 $\pm$ 0.5 ns (20°C) (*22*). Time-resolved fluorescence resulted in τ_R = 7 ns (20°C) (*22*). Hydrodynamic calculations which do not explicitly account for the bound water provide τ_R = 4.69 ns (*23*) and 5.95 ns (*24*). However, the same calculations provide translation diffusion rates which are respectively 20 and 10% higher than the experimental value (1.06 $\pm$ 0.01 $\times$ 10^6 cm^2/s) (*22*). This mismatch can be alleviated if some reasonable water shell is included. In this case, the overall-rotation correlation time is expected to rise to about 8–10 ns. Thus it is still not clear if τ_R can be independently obtained using another experimental technique with the accuracy required for the heteronuclear studies of the protein dynamics.

Here we elucidate what results would be observed if regular formal analysis, using τ_R estimated from the $R(S_x)/R(S_z)$ ratio, is applied to the protein involved in the internal motions on the nanosecond time scale. Since the majority of NMR relaxation studies on proteins published to date were performed at one magnetic field strength, we consider this situation first. ^{15}N relaxation rates and NOEs were simulated for a spherical molecule with a τ_R of 6 ns (Eq. [5]) involved in the nanosecond motions of substantial amplitude (S_s = 0.6, 0.8) (Eq. [4b]). Then the data were processed on the assumption of fast I and fast II models of internal motions (Eqs. [3]). The results of the fit are shown in Fig. 1. It is clear from Fig. 1 that neither the statistical criterion based on the value of the χ^2 loss function (Fig. 1a) nor the NOE values (Fig. 1b) can detect the presence of nanosecond motions with correlation time τ_s longer than 1.5–2.0 ns. Namely if τ_s is longer than 1.5–2 ns, NOEs have relatively high positive values and approach their theoretical upper limit with further increases in τ_s. The χ^2 loss function drops below its critical value if τ_s is longer than 4.0–4.5 and 1.5–2.0 ns for fast II and fast I models, respectively. In this case, on the basis of the statistical criterion, one would erroneously adopt fast models for the following data analysis. One should note that in this case relatively short $(\tau_e)_{app}$ obtained using the fast II model (Fig. 1d) also does not contradict this choice. Uncertainties in the ''experimental'' data higher than those used in the calculations (2% for $R(S_x)$ and $R(S_z)$, 3% for NOEs) would result in a uniform decrease of the χ^2 function and consequently even poorer model discrimination. We also tried to get τ_R as a free parameter in the fit of the same simulated relaxation data to fast I and fast II models (data not shown). For $\tau_s < 0.5$ ns apparent $(\tau_R)_{app}$ values obtained in this way using the fast I model are closer

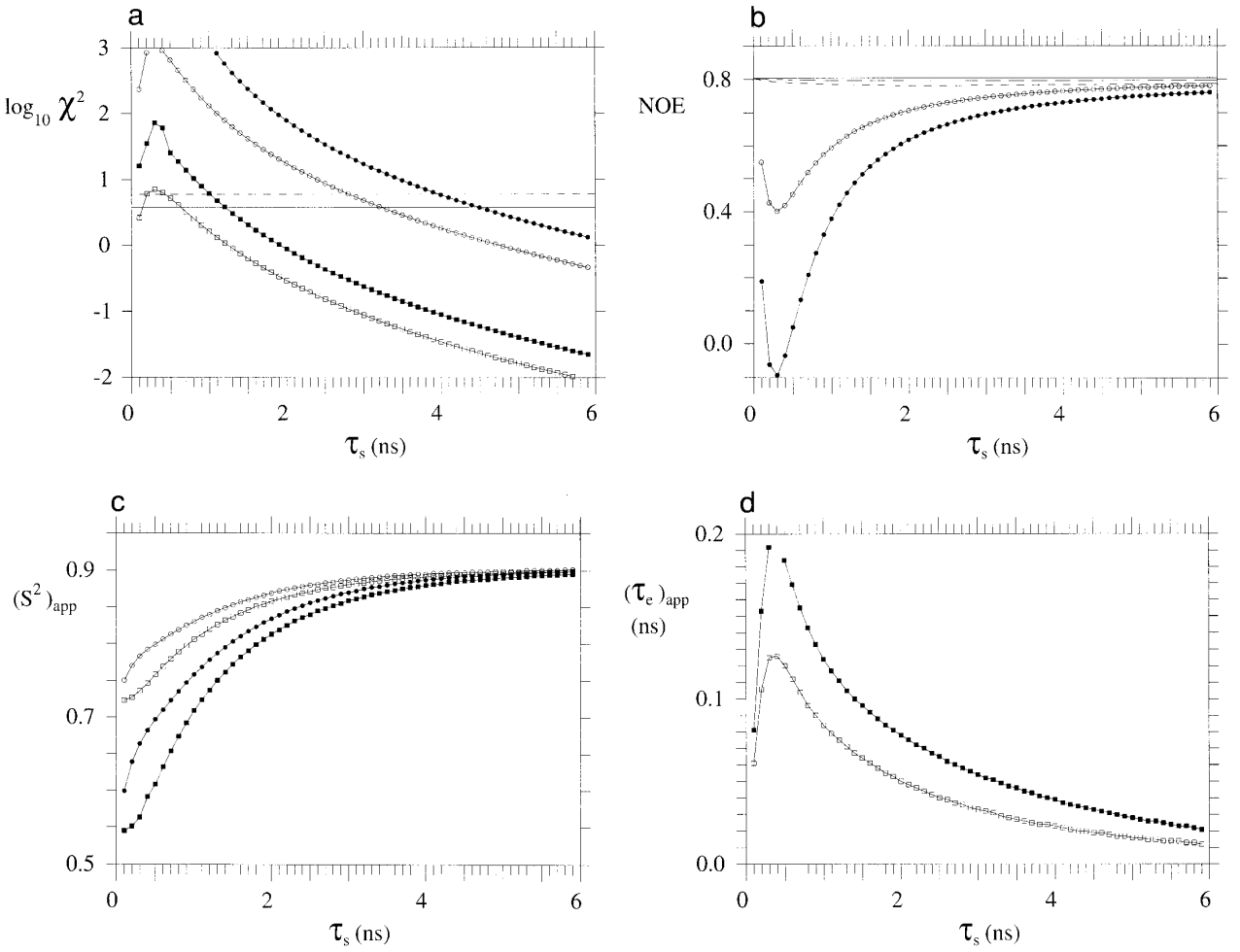

FIG. 1. Results of the formal model-free analysis of 600 MHz (^{1}H) relaxation data simulated for the molecule exhibiting internal motions on the nanosecond time scale. Relaxation data were simulated for a spherical molecule (τ_R = 6 ns) using the ''nanosecond'' model of internal motions (Eqs. [2], [4b], and [5]) with S_f^2 = 0.9. Order parameters, S_s^2, of 0.6 and 0.8 correspond to filled and open signs in plots, respectively. Data were fitted using ''fast I'' (Eq. [3a]) and ''fast II'' (Eq. [3b]) models of internal motions (squares and circles in plots, respectively) and the isotropic model of overall rotation (Eq. [5]). Apparent $(\tau_R)_{app}$ values obtained from $R(S_x)/R(S_z)$ ratios were utilized in the fit. All values are plotted versus the correlation time of nanosecond internal motions, τ_s in Eq. [4b]. (a) Logarithm of χ^2 loss function. Five percent probability critical levels for the models represented by Eq. [3a] and Eq. [3b] are shown by horizontal dashed and solid lines, respectively. (b) Simulated ^{15}N–^{1}H NOE values (open and filled circles). Maximal NOE for exact τ_R (solid line) and apparent $(\tau_R)_{app}$. $(\tau_R)_{app}$ were calculated from $R(S_x)/R(S_z)$ ratios for S_s^2 = 0.6 (short dashed line) and 0.8 (long dashed line), respectively. (c) Apparent order parameters $(S^2)_{app}$. Note that for the long τ_s, order parameters $(S^2)_{app}$ almost exactly reproduce the value of S_f^2 = 0.9. (d) Apparent correlation times of the internal motions $(\tau_e)_{app}$.

to the exact value than those from the $R(S_x)/R(S_z)$ ratio. However, for $\tau_s > 1.5–2$ ns, both methods provide almost the same underestimated $(\tau_R)_{app}$ values. Therefore, the regular analysis of relaxation data completely fails to detect nanosecond internal motions with characteristic times longer than 1.5–2.0 ns.

If exact τ_R is utilized in the model-free analysis (data not shown), fast II and fast I models provide χ^2 values which are significantly higher than critical values; i.e., the statistical criterion allows selection of the adequate model. This means that independent and precise measurement of τ_R would be very helpful for discrimination between models of internal motions. If only a limited number of amide groups in the molecule are involved in the nanosecond motions, with most of the molecule exhibiting fast motions, good estimates of τ_R can be obtained in a regular way from the averaged $R(S_x)/R(S_z)$ ratio. This provides validation for the application of the commonly used model-free analysis for such cases.

Fortunately, for relatively long τ_s, erroneously chosen fast II or fast I models provide order parameters which can be readily interpreted as the order parameters of picosecond motions. Namely, with increase of τ_s, the calculated order parameters, $(S^2)_{app}$, approach the exact order parameters of fast internal motions, S_f^2 (Fig. 1c). For τ_s longer than 3–4

ns $(S^2)_{app}$ values match S_f^2 within the experimental errors. Thus it is not surprising that the order parameters obtained in the $^{15}N-^{1}H$ NMR studies correspond well to the results of subnanosecond molecular-dynamics simulations (*25–27*). However, longer MD simulations (*19*) revealed poor correspondence with the order parameters derived from NMR data. Namely, 1 ns MD-derived order parameters were lower than experimental (*19*). Besides, Smith *et al.* (*19*) noted that even the 1 ns MD simulation was far from a complete sampling of the motions on the nano–picosecond time scale.

The relaxation data measured at several magnetic field strengths provide additional information to test the validity of the applied dynamic model. From Eq. [3] it follows that for fast I (S^2, τ_e) and fast II (S^2) dynamic models, the experimental $R(S_z)$ (lower field)/$R(S_z)$ (higher field) ratio should not depend on the parameters of internal motions, and can be predicted using $(\tau_R)_{app}$ calculated from the $R(S_x)/R(S_z)$ ratio. In the ^{15}N relaxation study of calcium-free calmodulin, Tjandra *et al.* (*28*) found that throughout the protein, experimental ratios of $R(S_z)$ (lower field)/$R(S_z)$ (higher field) were systematically lower than anticipated. This effect was attributed to the segmental motions on the nanosecond time scale in the protein. It is known, however, that the ratio of longitudinal relaxation rates measured at different magnetic fields is also extremely sensitive to the settings of the CSA constant, of which the proper value for the protein amides is not yet clear (*29*). This diminishes the merits of this ratio as an unambiguous criterion of the existence of nanosecond internal motions.

Calculation shows that the apparent $(\tau_R)_{app}$ derived from the $R(S_x)/R(S_z)$ ratio for different magnetic field strengths is most insensitive to reasonable deviations from the generally accepted $^{15}N-^{1}H$ distance and CSA value. However, the value of $(\tau_R)_{app}$ depends significantly on the magnetic field strength if there are motions on the nanosecond time scale. The dependencies of the apparent $(\tau_R)_{app}$ on the correlation time of internal motions are illustrated in Fig. 2. The shortest $(\tau_R)_{app}$ is found for τ_s of about 2 ns, where $(\tau_R)_{app}$ can be 10% less than the exact value even for the moderate amplitudes of the motions ($S_s^2 = 0.8$) (Fig. 2a). The minima become deeper with lower S_s^2 and longer τ_R. For comparison the same effect is shown in Fig. 2b for $^{1}H-^{13}C^{\alpha}$. As was noted by Kay *et al.* (*6*) in the case of $^{1}H-^{13}C$ relaxation, the $R(S_x)/R(S_z)$ ratio cannot be used for the determination of the overall-rotation correlation time, since even fast picosecond motions (τ_e of 10–50 ps) could significantly bias the apparent $(\tau_R)_{app}$ from its real value.

It is notable that the difference between the apparent $(\tau_R)_{app}$ values obtained at different spectrometer fields is particularly sensitive to the nanosecond time scale motions. Usually $(\tau_R)_{app}$ for proteins is reported with a precision of 0.02–0.1 ns [e.g., see (*5, 30*)]. Therefore, the difference of 0.1–0.5 ns in the apparent $(\tau_R)_{app}$, obtained from the $R(S_x)/R(S_z)$ ratio on the different magnetic field strengths, is statistically meaningful and can serve as a reason to reject models of fast internal motions. Indeed Orekhov *et al.* (*8*) observed the difference between $(\tau_R)_{app}$ derived from $^{1}H-^{15}N$ relaxation measurements at spectrometer frequencies of 400 and 600 MHz (^{1}H) for fragment 1–36 of bacterioopsin and attributed this effect to motions in the nanosecond time scale.

It can be shown that phenomena other than nanosecond internal motions can hardly contribute to the difference between apparent $(\tau_R)_{app}$ at different spectrometer frequencies. First, the apparent $(\tau_R)_{app}$ would be longer than anticipated on the spectrometer with a higher field for the residues involved in the conformational exchange (''chemical exchange'') in the micro–millisecond time scale. Since this effect has a sign opposite to that of nanosecond motions, it could not lead to incorrect rejection of the fast models.

The anisotropy of overall rotation is also known to change the apparent $(\tau_R)_{app}$ (*24, 31*). Therefore, one could expect that it can give rise to the relationship between apparent $(\tau_R)_{app}$ and the magnetic field strength. Below we elucidate the dependence of the apparent $(\tau_R)_{app}$ on the magnetic field strength that one can expect due to anisotropy of molecular rotation. The apparent τ_R was generated from $R(S_x)/R(S_z)$ ratios at several spectrometer fields for a rigid axially symmetric anisotropic molecule (Eqs. [6], [7]). A θ of 90° was used for the model calculations since this value provides the greatest dependence of $(\tau_R)_{app}$ on the spectrometer field. At the first step, the degree of molecular anisotropy $D_\parallel/D_\perp$ was fixed to 2.5 and the apparent $(\tau_R)_{app}$ was generated from $R(S_x)/R(S_z)$ versus the effective overall correlation time τ_R (Eq. [7]). Results presented in Fig. 3a show that the maximal difference in $(\tau_R)_{app}$ derived from the $R(S_x)/R(S_z)$ ratio at different spectrometer fields was found for molecules with an effective overall correlation time τ_R (Eq. [7]) close to 3 ns. It is this value of the correlation time that was used in further considerations. At the second step, the ratios of the apparent $(\tau_R)_{app}$ at different spectrometer fields are calculated versus the degree of the molecule anisotropy, $D_\parallel/D_\perp$ (Fig. 3b). Results presented in Fig. 3 provide the upper limit of the $(\tau_R)_{app}$ field dependence, which does not exceed 2% between 400 and 750 MHz (^{1}H) for regular globular protein with $0.4 \leqslant D_\parallel/D_\perp \leqslant 1.8$ and an effective rotation correlation time τ_R on the nanosecond time scale.

As can be seen in Fig. 2, $(\tau_R)_{app}$ is the most field dependent if internal motions have correlation times near 2.5–3 ns, providing a product with ^{15}N angular resonance frequency, $\omega\tau_s \sim 1$. In other words, $(\tau_R)_{app}$ would strongly depend on the magnetic field if the spectral density function can be approximated by the sum of at least two Lorentzians. One of these Lorentzians should have a correlation time close to 3 ns. The other must have a significantly longer correlation time. The above conditions could be fulfilled for a protein commonly elucidated by high-resolution NMR exhibiting an overall-rotation correlation time of about 5–10 ns, provided that it is involved in the motions on the nanosecond time

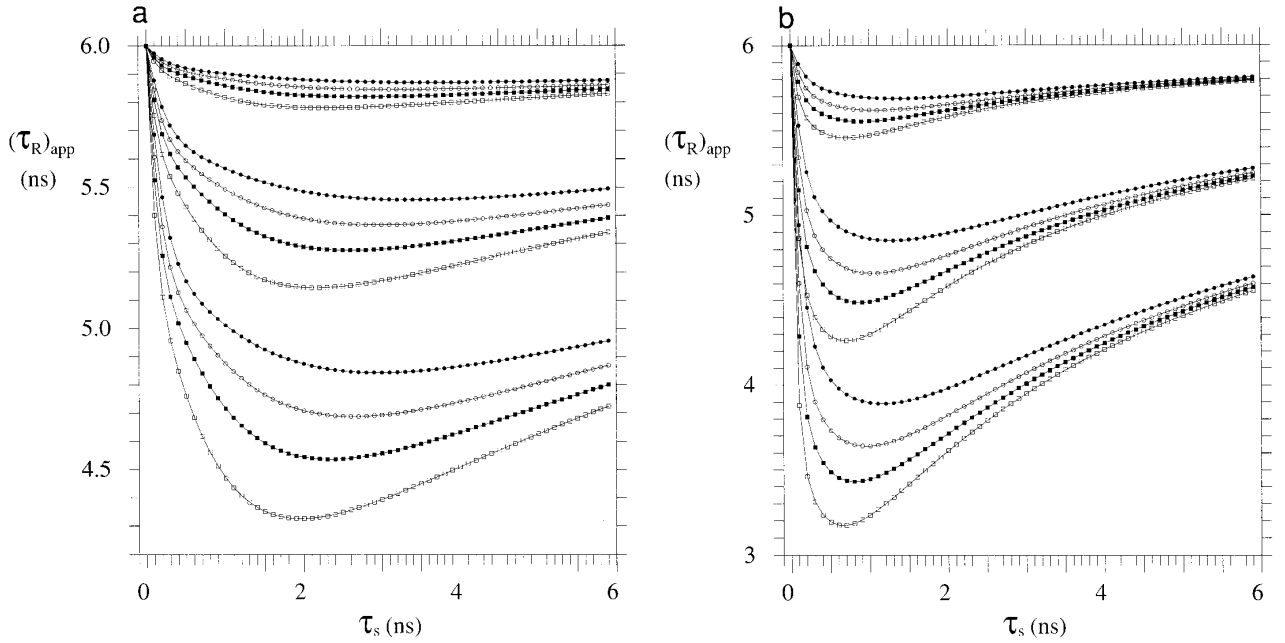

FIG. 2. Apparent overall-rotation correlation time $(\tau_R)_{app}$ calculated from the $R(S_x)/R(S_z)$ ratio as a function of the correlation time of the nanosecond internal motions, τ_s (Eq. [4b]). Relaxation rates $R(S_x)$ and $R(S_z)$ were simulated for a spherical molecule ($\tau_R = 6$ ns) using the ''nanosecond'' model of internal motions (Eqs. [2], [4b], and [5]) with $S_f^2 = 0.9$. Three sets of curves from the top to the bottom correspond to three values of the order parameter $S_s^2 = 0.95$, 0.8, and 0.6, respectively. In each set dependencies are shown for the four spectrometer frequencies (^{1}H): 400, 500, 600, and 750 MHz corresponding to filled circles, open circles, filled squares, and open squares, respectively. (a) Data for the ^{15}N–^{1}H vector. (b) Data for the $^{13}C^{\alpha}$–^{1}H vector.

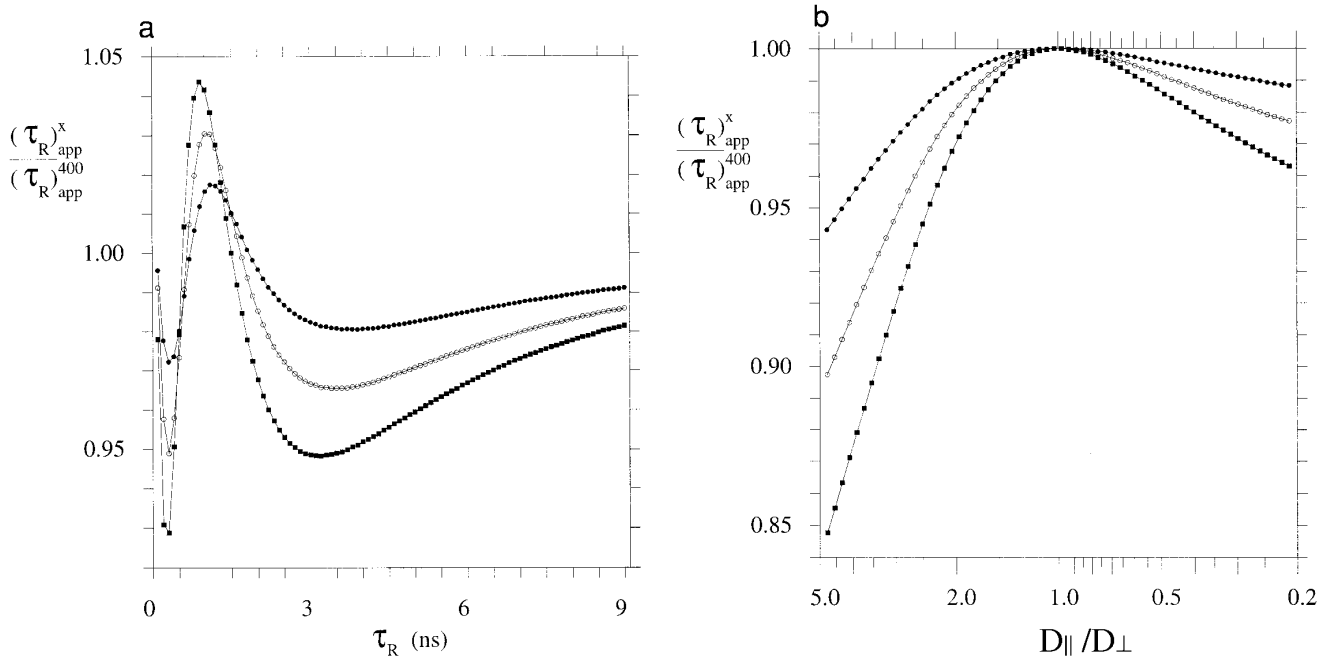

FIG. 3. Ratio of apparent overall-rotation correlation times $(\tau_R)^x_{app}/(\tau_R)^{400}_{app}$ calculated from $R(S_x)/R(S_z)$ ratios for a set of magnetic fields, for frequencies of 500, 600, and 750 MHz (^{1}H), corresponding respectively to filled circles, open circles, and filled squares. Relaxation rates $R(S_x)$ and $R(S_z)$ were simulated for a rigid anisotropic symmetric top molecule using Eqs. [2], [3b], [6], and [7]. (a) The $(\tau_R)^x_{app}/(\tau_R)^{400}_{app}$ ratio is shown versus the exact overall-rotation correlation time τ_R (Eq. [7]) for $D_\parallel/D_\perp = 2.5$. (b) The $(\tau_R)^x_{app}/(\tau_R)^{400}_{app}$ ratio is shown versus the $D_\parallel/D_\perp$ ratio. Overall-rotation correlation time τ_R is 3 ns.

scale. However, physical processes introducing Lorentzians with greater correlation times, e.g., protein association, do not lead to significant $(\tau_R)_{app}$ field dependence. Thus calculations show that the $(\tau_R)_{app}$ difference at 750 and 400 MHz (^{1}H) due to dimerization of the protein with the monomer overall correlation time of about 6 ns does not exceed 2.3% for any population of the protein in the dimer and monomer states. Consequently, a dependence of the apparent $(\tau_R)_{app}$ on magnetic field strength should be treated as evidence of the substantial internal motions on the nanosecond time scale.

CONCLUSIONS

We considered the complications arising in ^{1}H$-^{15}$N NMR dynamic studies due to internal dynamics on the nanosecond time scale. In particular, the regular approach using the overall-rotation correlation time calculated from the $R(S_x)/R(S_z)$ ratio is not capable of detecting motions with correlation times longer than 1.5–2 ns if these motions involve most of the protein. These motions can be properly quantified if relaxation data at several spectrometer frequencies are available or if the overall-rotation correlation time is known from independent measurements. It is shown however that even in the cases of complex dynamics on the nanosecond time scale, the internal dynamics on the picosecond time scale can be adequately quantified using the effective overall-rotation correlation times. These effective rotation correlation times should be individually calculated for the particular ^{1}H$-^{15}$N vectors from the $R(S_x)/R(S_z)$ ratio. A new criterion for the detection of nanosecond motions is introduced. Namely it is shown that the observation of a significantly lower apparent overall-rotation correlation time on the spectrometer with a higher magnetic field unambiguously indicates motions on the nanosecond time scale. Our conclusions question whether the majority of previous ^{1}H$-^{15}$N NMR model-free dynamic studies can be regarded only as a rough characterization of the picosecond protein dynamics, and whether their results should be reinterpreted in favor of the presence of the nanosecond motions.

ACKNOWLEDGMENTS

This research was supported by grants from the Russian Foundation of Basic Research (96-04-50893, 00054), Russian State Science and Technology Program Grant 03.000H, and ISSEP Grant a96-269.

REFERENCES

1. G. Lipari and A. Szabo, *J. Am. Chem. Soc.* **104,** 4546–4559 (1982).
2. G. Lipari and A. Szabo, *J. Am. Chem. Soc.* **104,** 4559–4570 (1982).
3. G. M. Clore, A. Szabo, A. Bax, L. E. Kay, P. C. Driscoll, and A. M. Gronenborn, *J. Am. Chem. Soc.* **112,** 4989–4991 (1990).
4. M. J. Stone, W. J. Fairbrother, A. G. Palmer, J. Reizer, M. H. Saier, and P. E. Wright, *Biochemistry* **31,** 4394–4406 (1992).
5. A. M. Mandel, M. Akke, and A. G. Palmer, *J. Mol. Biol.* **246,** 144–163 (1995).
6. L. E. Kay, D. A. Torchia, and A. Bax, *Biochemistry* **28,** 8972–8979 (1989).
7. D. E. Woessner, *J. Chem. Phys.* **37,** 647–654 (1962).
8. V. Yu. Orekhov, K. V. Pervushin, D. M. Korzhnev, and A. S. Arseniev, *J. Biomol. NMR* **6,** 113–122 (1995).
9. A. G. Palmer, M. Rance, and P. E. Wright, *J. Am. Chem. Soc.* **113,** 4371–4380 (1991).
10. J. M. Schurr, H. P. Babcock, and B. S. Fujimoto, *J. Magn. Reson.* **105,** 221–224 (1994).
11. D. E. Woessner, *J. Chem. Phys.* **35,** 41–48 (1961).
12. A. Abragam, ''The Principles of Nuclear Magnetism,'' Oxford Univ. Press, London (1961).
13. R. King and O. Jardetzky, *Chem. Phys. Lett.* **55,** 15–18 (1978).
14. O. Jardetzky and G. C. Roberts, ''NMR in Molecular Biology,'' Academic Press, New York (1981).
15. V. Yu. Orekhov, D. E. Nolde, A. P. Golovanov, D. M. Korzhnev, and A. S. Arseniev, *Appl. Magn. Reson.* **9,** 581–588 (1996).
16. F. Cordier, B. Bernhard, and D. Marion, *J. Biomol. NMR* **7,** 163–168 (1996).
17. L. Zeng, M. W. Fischer, and E. R. Zuiderweg, *J. Biomol. NMR* **7,** 157–162 (1996).
18. A. J. Wand, J. L. Urbauer, R. P. McEvoy, and R. J. Bieber, *Biochemistry* **35,** 6116–6125 (1996).
19. L. J. Smith, A. E. Mark, C. M. Dobson, and W. F. van Gunsteren, *Biochemistry* **34,** 10918–10931 (1995).
20. J. F. Lefevre, K. T. Dayie, J. W. Peng, and G. Wagner, *Biochemistry* **35,** 2674–2686 (1996).
21. M. Buck, J. Boyd, C. Redfield, D. A. MacKenzie, D. J. Jeenes, D. B. Archer, and C. M. Dobson, *Biochemistry* **34,** 4041–4055 (1995).
22. S. B. Dubin, N. A. Clark, and G. B. Benedek, *J. Chem. Phys.* **14,** 5138–5164 (1971).
23. R. M. Venable and R. W. Pastor, *Biopolymers* **27,** 1001–1014 (1988).
24. D. Brune and S. Kim, *Proc. Natl. Acad. Sci. USA* **90,** 3835–3839 (1993).
25. M. A. L. Eriksson, H. Berglund, T. Hard, and L. Nilsson, *Proteins* **17,** 375–390 (1993).
26. J. Kordel and O. Teleman, *J. Am. Chem. Soc.* **114,** 4934–4936 (1992).
27. A. G. Palmer and D. A. Case, *J. Am. Chem. Soc.* **114,** 9059–9067 (1992).
28. N. Tjandra, H. Kuboniwa, H. Ren, and A. Bax, *Eur. J. Biochem.* **230,** 1014–1024 (1995).
29. N. Tjandra, P. Wingfield, S. Stahl, and A. Bax, *J. Biomol. NMR* **8,** 273–284 (1996).
30. D. M. Epstein, S. J. Benkovic, and P. E. Wright, *Biochemistry* **34,** 11037–11048 (1995).
31. R. Brüschweiler, L. Xiubei, and P. E. Wright, *Science* **268,** 886–889 (1995).